CrystEngComm

PAPER

View Article Online
View Journal | View Issue

CrossMark
click for updates

Cite this: *CrystEngComm*, 2015, **17**, 5389

1D iron(II) spin crossover coordination polymers with 3,3′-azopyridine – kinetic trapping effects and spin transition above room temperature†

Sophie Schönfeld, Charles Lochenie, Peter Thoma and Birgit Weber*

Received 23rd April 2015,
Accepted 19th May 2015

DOI: 10.1039/c5ce00800j

www.rsc.org/crystengcomm

Two new iron(II) 1D coordination polymers with spin crossover behaviour were synthesised using 3,3′-azopyridine as bridging axial ligand and N_2O_2 coordinating Schiff base-like equatorial ligands. The X-ray structures of both complexes were solved revealing very different packing patterns for the two complexes. Magnetic measurements reveal a spin transition with hysteresis and kinetic trapping effects at lower temperatures for one complex and a spin transition above room temperature for the second complex.

Introduction

Iron(II) spin crossover (SCO) complexes belong to a very actively investigated class of switchable molecular materials. The transition between the paramagnetic high spin (HS, S = 2) and the diamagnetic low spin (LS, S = 0) state can be triggered by many different possibilities.[1] Additionally these complexes can be nanostructured,[2] incorporated into composite materials[3] or can be combined with additional properties.[4] These lead to a very wide application potential for this kind of complexes in the field of sensing or data storage. From the application point of view, abrupt spin transitions (that take place in the range of a few K) or spin transitions with hysteresis (with different transition temperatures $T_{1/2}$ in the heating and the cooling modes) are especially desirable. For some of these complexes with cooperative spin transition, the scan rate used for the magnetic measurement can influence the observed width of the thermal hysteresis loop. A very pronounced scan rate dependence was recently reported for a dinuclear iron(II) spin crossover complex[5] and a mononuclear cobalt(II) complex,[6] both showing a spin transition with hysteresis. Often phase transitions are responsible for a pronounced scan rate dependence of the width of the thermal hysteresis loop. A very impressive example, where depending on the scan rate different LS states with different metastable HS states were obtained, was presented by Real and coworkers.[7] Another kinetic effect can be observed, if the thermal spin transition takes place at rather low temperatures. In this case the interplay between a kinetically slow thermal spin transition and the relaxation from the metastable HS state is possible.[8,9]

For the spin crossover complexes investigated by our group, the observation of kinetic effects is rare. Routinely, we present the results of the magnetic measurements in settle mode to allow a better comparison of the different substances.[10] However, the first characterisation of the magnetic properties of a new compound is normally done in sweep mode (usually with a rate of 5 K min^{-1}) and in most of the cases no significant differences between the two curves are observed. So far there is only one example for a kinetic trapping effect (close $T_{1/2}$ and T_{LIESST}) observed for a 1D chain complex synthesised by our group.[11] Here we present two new 1D chain coordination polymers of the Schiff base-like ligands used by our group and 3,3′-azopyridine as bridging axial ligand. While one of the two complexes shows a spin transition above room temperature, for the second complex pronounced kinetic effects are observed. The differences in the magnetic properties can be related to the differences in the crystal packing of these two complexes.

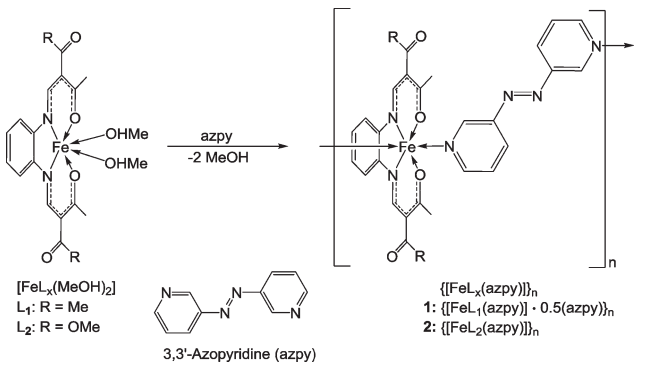

Scheme 1 General synthesis of the iron(II) coordination polymers **1** and **2**.

Inorganic Chemistry II, University of Bayreuth, Universitätsstr. 30, 95440 Bayreuth, Germany. E-mail: weber@uni-bayreuth.de; Tel: +49(0)921 55 2555

† Electronic supplementary information (ESI) available. CCDC 1053319 1053320. For ESI and crystallographic data in CIF or other electronic format see DOI: 10.1039/c5ce00800j

Open Access Article. Published on 22 May 2015. Downloaded on 8/18/2024 12:57:07 AM.
This article is licensed under a Creative Commons Attribution 3.0 Unported Licence.

Open Access Article. Published on 22 May 2015. Downloaded on 8/18/2024 12:57:07 AM.
This article is licensed under a Creative Commons Attribution 3.0 Unported Licence.

Results

Synthetic procedures

The octahedral iron(II) 1D coordination polymers were obtained in a one-pot reaction using the related mononuclear methanol complexes as starting materials.[12,13] A ligand substitution reaction with the bridging ligand 3,3′-azopyridine[14,15] gave complexes $\{[FeL1(azpy)]\cdot 0.5(azpy)\}_n$ (**1**) and $\{[FeL2(azpy)]\}_n$ (**2**) in good yields. Scheme 1 displays the general synthesis of the iron(II) coordination polymers **1** and **2**. The complexes were fully characterised by elemental analysis, IR and mass spectrometry. Moreover X-ray diffraction data could be obtained for both complexes.

Single crystal X-ray structure analysis

Crystals suitable for X-ray structure analysis were obtained for **1** and **2** by using a slow diffusion technique at room temperature. The crystallographic data of **1** and **2** are summarized in Table S1.† The molecular structures of both compounds were determined at 133 K.

Complex **1** crystallises in monoclinic space group *C*2/*c*, with eight formula units in the unit cell. Fig. 1 displays the ORTEP drawing of the asymmetric unit together with the used atom numbering scheme. The asymmetric unit of **1** consists of one monomeric unit of the coordination polymer $\{[FeL1(azpy)]\}_n$ and half of a non-coordinating azpy molecule. This is in agreement with the composition obtained for the bulk material (see the Experimental section). The iron(II) centre has an octahedral coordination sphere consisting of the equatorially coordinated Schiff base-like ligand and the axially coordinated bridging ligand azpy, bound through terminal 3-pyridyl groups. Selected bond lengths and angles within the inner coordination sphere of both complexes **1** and **2** are summarized in Table 1. The bond lengths and angles within the inner coordination sphere of **1** are within the range reported for HS iron(II) complexes of this ligand type.[11,16,17] The average bond lengths are 2.02 Å ($Fe–O_{eq}$), 2.10 Å ($Fe–N_{eq}$) and 2.26 Å ($Fe–N_{ax}$). The average $O_{eq}–Fe–O_{eq}$ angle is 110.58(9)° clearly in the range typical for the HS state.[11,16,17] The $N_{ax}–Fe–N_{ax}$ angle (173.18(10)°) does not differ significantly from the expected 180° for an ideal octahedron.

Table 1 Selected bond lengths [Å] and angles [degree] within the inner coordination sphere of the iron(II) coordination polymers with the ligand system H_2L1 and H_2L2. The X-ray structures were determined at 133 K

	$Fe–N_{eq}$	$Fe–O_{eq}$	$Fe–N_{ax}$	$O_{eq}–Fe–O_{eq}$	$N_{ax}–Fe–N_{ax}$
1	2.098(3) 2.109(3)	2.019(2) 2.024(2)	2.257(3) 2.266(3)	110.58(9)	173.18(10)
2	1.903(2) 1.893(2)	1.9341(19) 1.9322(19)	1.997(2)	88.74(7)	174.91(9)

Complex **2** crystallizes in triclinic space group P$\bar{1}$, with two formula units in the unit cell. Fig. 2 displays the ORTEP drawing of the complex together with the atomic numbering scheme. The asymmetric unit consists of one monomeric unit of the coordination polymer $\{[FeL2(azpy)]\}_n$. The bond lengths and angles of the inner coordination sphere of **2**, displayed in Table 1, are within the range reported for a octahedral LS iron(II) complex of this ligand type.[11,16,17] The average bond lengths are 1.90 Å ($Fe–O_{eq}$), 1.93 Å ($Fe–N_{eq}$) and 2.00 Å ($Fe–N_{ax}$). Based on the $O_{eq}–Fe–O_{eq}$ angle it is possible to make a statement about the spin state of the iron centre. For this complex the average angle is 89° clearly in the range typical for the LS state.[11,16,17] The $N_{ax}–Fe–N_{ax}$ angle (174.91(9)°) does not differ significantly from the expected 180° for an ideal octahedron.

Table 2 gives the selected bond lengths between the carbon atoms of the Schiff base-like ligand for both compounds. The average bond length of 1.43 Å cannot be attributed to a single or double bond, showing that the negative charge of the nitrogen is therefore delocalized over the chelate ring.

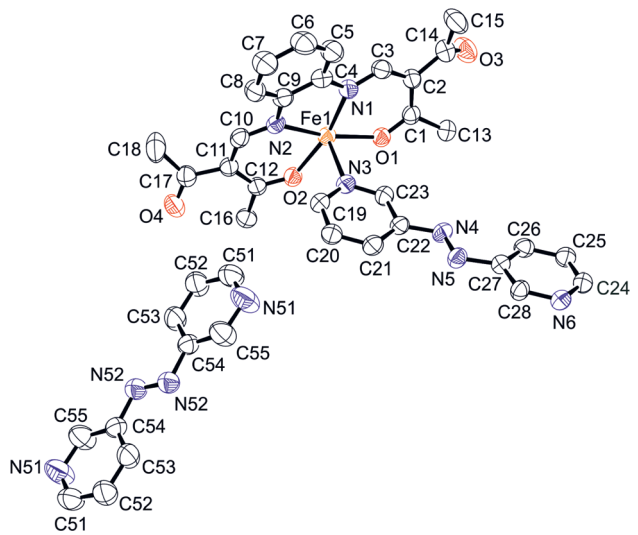

Fig. 1 ORTEP drawing of the asymmetric unit of **1** with the atom numbering scheme used in the text. Hydrogen atoms are omitted for clarity. Thermal ellipsoids presented at 50% level.

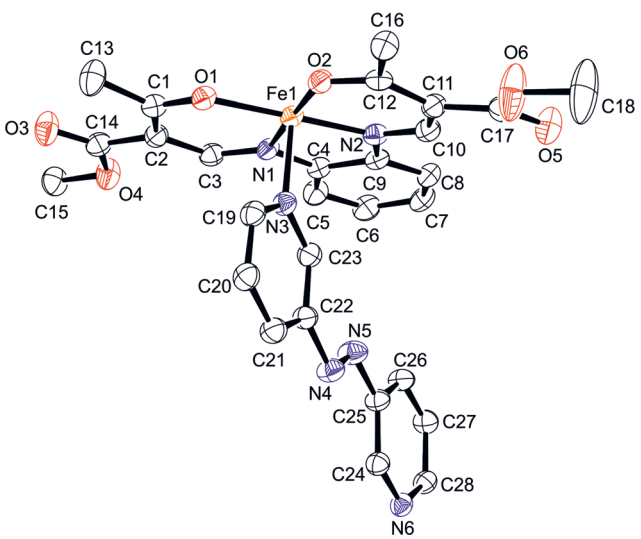

Fig. 2 ORTEP drawing of the asymmetric unit of **2** with the atom numbering scheme used in the text. Hydrogen atoms are omitted for clarity. Thermal ellipsoids presented at 50% level.

This journal is © The Royal Society of Chemistry 2015

Open Access Article. Published on 22 May 2015. Downloaded on 8/18/2024 12:57:07 AM.
This article is licensed under a Creative Commons Attribution 3.0 Unported Licence.

Table 2 Selected bond lengths [Å] and torsion angles [degree] of the iron(II) coordination polymers discussed in this work

	C(1)–C(2)	C(2)–C(3)	C(10)–C(11)	C(11)–C(12)	Atoms	Torsion angle
1	1.423(5)	1.419(5)	1.413(5)	1.430(4)	C(22)–N(4)–N(5)^a–C(27)^a	178.1(3)
					C(54)–N(52)–N(52)^b–C(54)^b	180.0(3)
2	1.427(4)	1.416(3)	1.424(3)	1.430(3)	C(22)–N(4)–N(5)–C(25)	179.9(2)

^{a} 1/2 + x, −1/2 + y, z. ^{b} 3/2 − x, 3/2 − y, 2 − z.

The comparison of the torsion angles (Table 2) between the coordinating azpy molecule and the non-coordinating azpy of **1** reveals that the coordinating molecule is bent whereas the non-coordinating one is ideally flat as expected for a sp^2 hybrid system. By connecting the two iron(II) centers the molecule is slightly bent and therefore the torsion angles differ from the expected 180°. However, this impact is not as pronounced for the bridging azpy molecules of **2**. Here the torsion angle corresponds to that of an ideally flat molecule and there appears to be less strain in the system.

In Fig. 3, the packing of the chains in the crystal of compound **1** is displayed. The 1D chains of **1** exhibit a zigzag motif. Chains that propagate in the same direction are linked by a hydrogen bond between the coordinating and the non-coordinating azpy (C55–H55···N5). The relevant intermolecular distances are summarized in Table 3. The 1D chains in combination with the hydrogen bonds form a 2D plane. The planes themselves are again linked by hydrogen bonds, on the one hand directly between the complexes (C8–H8···O3, C25–H25···O4) and on the other hand through the non-coordinating azpy (C52–H52···O4). These specific linkages are responsible for the unique perpendicular orientation of the chains. Interestingly, such a perpendicular arrangement of the 1D chains was also observed for related 4,4′-azopyridine-based coordination polymers,[18,19] whereas for other coordination polymers of this ligand type, only parallel aligned 1D chains were obtained so far.[16]

In contrast to **1**, in the crystal packing of **2**, the 1D chains propagate parallel along the [1 0 0] direction and are stacked such that the unit cell contains no residual solvent-accessible void volume (Fig. 4). The parallel 1D chains are linked by a hydrogen bond between the coordinating azpy and the oxygen of the ester group of the equatorial ligand (C27–H27···O5, see Table 3). The 1D chain of **2** exhibits also a slight zigzag motif due to the *trans*-arrangement of the coordinating nitrogen atoms in the ligand.

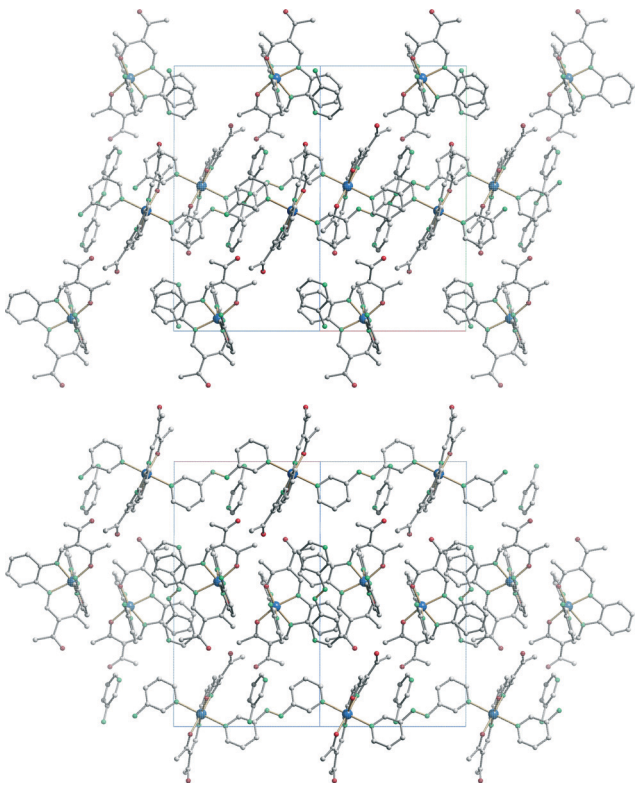

Fig. 3 Molecular packing of compound **1** in the crystal at 133 K. Top: view along [−1 1 0] and bottom: view along [1 1 0]. The hydrogen atoms have been omitted for clarity.

Magnetic measurements

Magnetic susceptibility measurements in the temperature range from 300/400 K to 10 K were undertaken to follow the iron(II) spin state change for the two samples.

The thermal dependence of the $\chi_M T$ product for complex **1** with the "standard" scanning rate of 5 K min^{-1} showed indications of a kinetic trapping of the HS state. Therefore the compound was studied in sweep mode with different cooling rates (0.5, 2, 5, and 10 K min^{-1}). The results of these measurements are displayed in Fig. 5. At room temperature, the compound has a $\chi_M T$ product of 3.21 cm^3 K mol^{-1}, in the typical range for iron(II) complexes in the HS state. Upon cooling with a rate of 0.5 K min^{-1}, the $\chi_M T$ product remains constant until 90 K, where the compound undergoes an incomplete gradual spin crossover from HS to LS to attain a

Table 3 Selected classical and non-classical hydrogen bonds [Å] of **1** and **2**

	Donor–H···acceptor	D–H	H···A	D···A	D–H···A
1	C(8)–H(8)···O(3)^a	0.93	2.57	3.406(4)	150
	C(25)–H(25)···O(4)^b	0.93	2.44	3.221(4)	141
	C(52)–H(52)···O(4)	0.93	2.40	3.280(6)	158
	C(55)–H(55)···N(5)^c	0.93	2.51	3.440(6)	173
2	C(27)–H(27)···O(5)^d	0.95	2.56	3.261(3)	131

^{a} x, 2 − y, 1/2 + z. ^{b} x, 2 − y, −1/2 + z. ^{c} 3/2 − x, −1/2 + y, 3/2 − z. ^{d} 2 − x, 1 − y, 1 − z.

Open Access Article. Published on 22 May 2015. Downloaded on 8/18/2024 12:57:07 AM.
This article is licensed under a Creative Commons Attribution 3.0 Unported Licence.

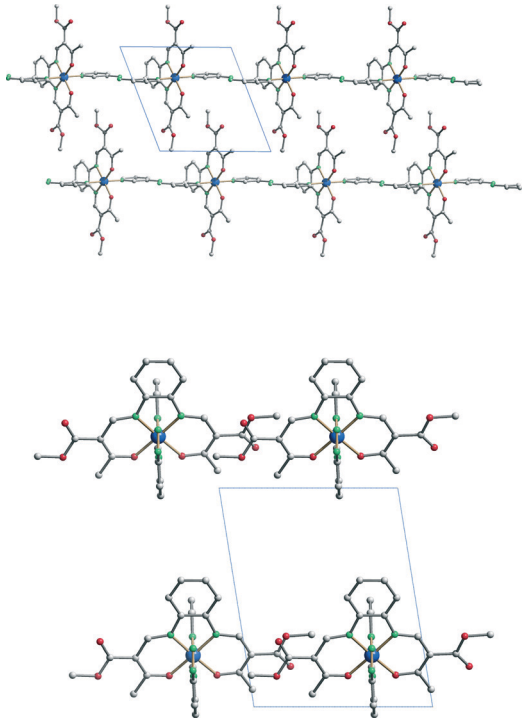

Fig. 4 Molecular packing of compound **2** in the crystal at 133 K. View along [0 0 1] (top) and [1 0 0] (bottom). The hydrogen atoms have been omitted for clarity.

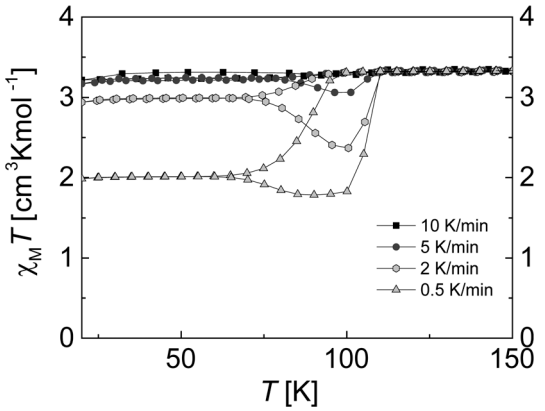

Fig. 5 Plot of the $\chi_M T$ product *vs.* T over the range 150–20 K with 10 K min^{-1} (squares), 5 K min^{-1} (filled circles), 2 K min^{-1} (open circles), 0.5 K min^{-1} (triangles) rates of cooling for the component **1**.

minimum $\chi_M T$ value of 1.78 cm^3 K mol^{-1}, indicative of a mixed HS(0.5)/LS(0.5) state. Such a plateau (remaining HS fraction) is often observed for coordination polymers of this ligand type with either a pronounced zigzag structure or a perpendicular arrangement of the 1D chains.[11,18,20]

The $\chi_M T$ product stays constant until 10 K. Upon heating, compound **1** exhibits a 15 K wide thermal hysteresis loop with critical temperatures of $T_{1/2}\downarrow$ = 90 K upon cooling and $T_{1/2}\uparrow$ = 105 K upon heating, coming back to a full HS state. By cooling down the component with a rate of 2 K min^{-1} a minimum $\chi_M T$ value of 2.37 cm^3 K mol^{-1} at 100 K can be observed, which is no longer in a range typical for a full HS iron(II) compound, nor for a mixed HS/LS state (74% of active sites remain trapped in the HS state). By increasing the cooling rate to 5 K min^{-1}, a minimum value of 3.06 cm^3 K mol^{-1} at 101 K is detected, showing that 95% of the active sites are trapped in the HS state. Finally, with a cooling rate of 10 K min^{-1}, the $\chi_M T$ values are constant within the whole temperature range and maintain a value of 3.21 cm^3 K mol^{-1}, showing that the HS state of the compound **1** is completely trapped.

Since complex **1** shows extraordinary thermal kinetic trapping, a TIESST (temperature induced excited spin state trapping) experiment was conducted (Fig. 6). The compound was rapidly cooled with a rate of 10 K min^{-1} from 300 K to 10 K. Using this procedure, the complex got trapped in a metastable HS state at 10 K. At this temperature the system would be in a mixed HS/LS form if a very slow cooling rate was used. The temperature is then slowly increased at a rate of 0.5 K min^{-1} and the magnetic behaviour is recorded. The magnetic response of the trapped high spin state remains relatively constant up to 60 K. Above 60 K the system reaches the thermally activated domain, and the HS → LS relaxation becomes more and more rapid to reach a minimum in the $\chi_M T$ *vs.* T curve at 85 K with a $\chi_M T$ value of 1.78 cm^3 K mol^{-1}, corresponding to the mixed HS/LS state. The critical temperature T_{TIESST} was found to be 73 K (the inset in Fig. 6). This is significantly higher than the T_{LIESST} temperatures observed so far for complexes of this ligand type (assuming that these temperatures are usually in the same order of magnitude). Upon further heating, the compound goes back to a full HS state at 105 K. In order to determine the actual width of the thermal hysteresis loop of **1** without any kinetic trapping effects, the complex was cooled from room temperature to a temperature between 80 K and 105 K (in intervals of 5 K) and

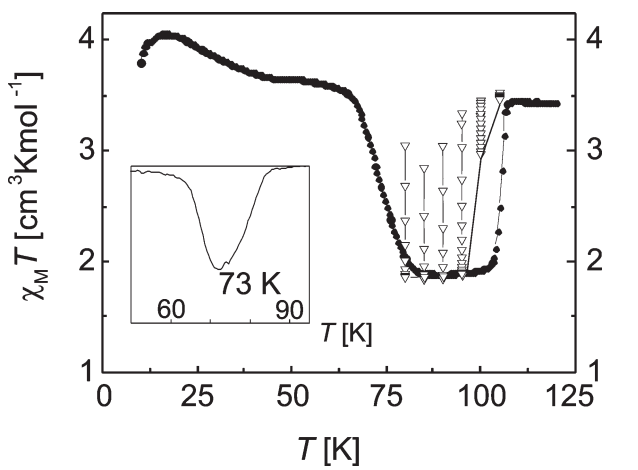

Fig. 6 Black cycles: TIESST experiment recorded for the coordination polymer **1** at a warming rate 0.5 K min^{-1}. The inset shows the first deviation for the determination of T_{TIESST}. Open triangles: relaxation of the thermally trapped HS state at 80, 85, 90, 95, 100 and 105 K for the determination of the hysteresis width without of trapping effects. The solid lines are guides for the eye.

This journal is © The Royal Society of Chemistry 2015

Open Access Article. Published on 22 May 2015. Downloaded on 8/18/2024 12:57:07 AM.
This article is licensed under a Creative Commons Attribution 3.0 Unported Licence.

then left at this temperature for the HS → LS relaxation (open triangles in Fig. 6). To follow the relaxation process, every 10 min a measurement point was taken. As illustrated in Fig. 6, full relaxation is observed up to a temperature of 95 K. At 100 K the system no longer relaxes completely into the mixed HS/LS state and at 105 K the complex remains in the HS state. This experiment shows that even with a sweeping velocity of 0.5 K min^{-1} kinetic effects influence the width of the hysteresis loop (determined to be 15 K) and the actual width excluding kinetic effects is more in the region of 7 K.

The thermal dependence of the $\chi_M T$ product of **2** is displayed in Fig. 7. The complex shows a gradual SCO between 350 and 400 K with a transition temperature of $T_{1/2}$ = 355 K to reach a maximum $\chi_M T$ value of 3.11 cm^3 K mol^{-1}, typical for an iron(II) complex in the HS state. Between 340 and 10 K the $\chi_M T$ values are approximately constant with a value close to zero (0.01 cm^3 K mol^{-1} at 10 K), which is typical for an iron(II) complex in the LS state.

Discussion

The two complexes **1** and **2** vary only in one substituent that has a marginal influence on the overall ligand field strength at the iron centre. Investigations into the spin transition behaviour in solution revealed almost identical transition temperatures.[16] Despite this, the spin transition behaviour, considering the transition temperature $T_{1/2}$, the completeness of the spin transition and the amount of cooperative interactions (hysteresis or not), of the two complexes is very different. This can only be due to the very different packing of the 1D chains in the crystal. The difference in the cooperative interactions (7 K wide hysteresis for **1** *vs.* gradual spin crossover for **2**) is probably the easiest to be explained. In contrast to **2** the packing of the molecules of **1** in the crystal (Fig. 3) reveals four different hydrogen bonds leading to 2D layers that are further interconnected. The hydrogen bonding of the free azpy molecules plays a decisive role. The additional azpy molecules in the packing of the complex cross-link these perpendicularly oriented chains that propagate in the same direction with a strong hydrogen bond (Table 3, hydrogen bond 4). In contrast to this, in the case of **2** only one non-classical hydrogen bond is observed. This significant difference in the amount of hydrogen bonds between the 1D chains easily explains the difference in the cooperative interactions. The magnetic characterisation for complex **1** shows an incomplete spin transition that stops at a plateau with about 50% of the molecules in the HS and 50% in the LS states while the SCO of **2** is complete. Two different reasons can be responsible for this observation. The first possibility is that only one out of the two planes propagating in perpendicular directions is undergoing the spin crossover. The second alternative, which was already observed for similar coordination polymers of this ligand type, is the formation of a mixed HS–LS chain with only every second iron centre undergoing spin transition due to restraining steric effects.[11] Both possibilities can explain the magnetic behaviour, resulting in a mixed HS/LS state. For **1**, intermolecular restraining interactions are easily imaginable because of the zigzag motif of the 1D chains in combination with the perpendicular orientation and the hydrogen bonds. All complexes characterised so far with such a perpendicular arrangement of 1D chains showed steps in the transition curve.[18] To provide assurance with regard to this hypothesis, it would be necessary to examine the X-ray diffraction data at low temperatures where the complex is in the mixed HS/LS state. Unfortunately the spin transition takes place at such low temperatures that it was not possible to obtain the desired data. The very low transition temperature of **1**, in combination with the intermolecular restraining interactions, also explains the trapping of the HS state during rapid cooling and the decreasing hysteresis width with slow cooling rates. Most likely the spin transition is accompanied by phase transitions (*e.g.* rearrangement of the H-bond network) leading to these kinetic effects. The complete spin transition of **2** and the weak cooperative effects are in good agreement in the presence of only one hydrogen bond linking the 1D chains that are, additionally, all parallel. Due to the high transition temperature (above room temperature) no kinetic trapping effects are observed.

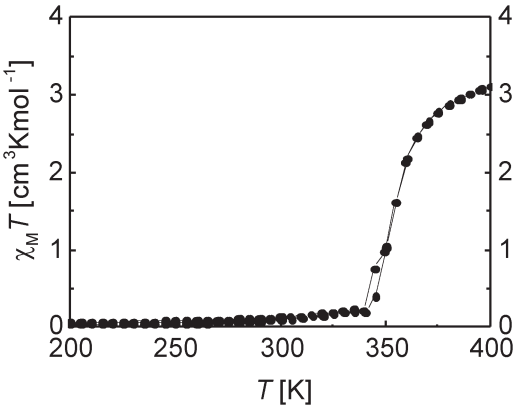

Fig. 7 Plot of the $\chi_M T$ product *vs.* T over the range 200–400 K for the compound **2**.

Experimental

Materials and methods

All syntheses were carried out under argon using Schlenk tube techniques. Methanol was dried over magnesium and distilled under argon before use. The syntheses of the starting complexes [FeL1/2$(MeOH)_2$] were prepared as described in the literature.[12,13] 3,3′-Azopyridine as an axial ligand was prepared according to the literature.[14,15]

{[FeL1(azpy)]·0.5(azpy)}$_n$ (1). A solution of [FeL1$(MeOH)_2$] (0.24 g, 0.54 mmol) and azpy (0.20 g, 1.08 mmol) in methanol (30 mL) was heated to reflux for 3 h. After cooling and left to stand at room temperature for 24 h, the precipitated black crystalline solid was filtered off, washed with methanol (2 × 5 mL) and dried *in vacuo* to give **1** (yield 0.24 g, 78.8%). **IR**

Open Access Article. Published on 22 May 2015. Downloaded on 8/18/2024 12:57:07 AM.
This article is licensed under a Creative Commons Attribution 3.0 Unported Licence.

(KBr): $\tilde{\nu}$ = 1638(s, ν[CO]), 1552(s, ν[N=N]); **MS** (DEI-(+), 70 eV): *m*/*z* (%): 382 (100) [FeL1$^+$], 367 (47) [M$^+$–Me], 184 (76) [azpy$^+$], 106 (46) [$C_5H_4N_3^+$], 78 (100) [$C_5H_4N^+$], 51 (37) [$C_4H_3^+$]. Elemental analysis calcd (%) for $C_{33}H_{30}FeN_8O_4$ (658.50 g mol^{-1}) C 60.19, H 4.59, N 17.02; found: C 60.52, H 4.48, N 17.07.

{[FeL2(azpy)]}$_n$ (2). A solution of [FeL2(MeOH)$_2$] (0.33 g, 0.69 mmol) and azpy (0.25 g, 1.38 mmol) in methanol (30 mL) was heated to reflux for 3 h. After cooling and left to stand at room temperature for 24 h, the black powder was filtered off, washed with methanol (6 mL) and dried *in vacuo* to give **2** (yield 0.3 g, 72.7%). **IR** (KBr): $\tilde{\nu}$ = 1688 (s, ν[CO]), 1557 (s, ν[N=N]), 1267 (vs, ν[C–O]); **MS** (DEI-(+), 70 eV): *m*/*z* (%): 414 (100) [FeL$_2^+$], 382 (29) [M$^+$–OCH$_3$], 340 (46) [M$^+$–COOMe$_2$], 309 (40) [$C_{14}H_9FeN_2O_3^+$], 184 (71) [azpy$^+$], 106 (46) [$C_5H_4N_3^+$], 78 (100) [$C_5H_4N^+$], 51 (39) [$C_4H_3^+$]. Elemental analysis calcd (%) for $C_{28}H_{26}FeN_6O_6$ (598.39 g mol^{-1}) C 56.20, H 4.38, N 14.04; found: 56.12, H 4.04, N 13.98.

X-ray diffraction

The intensity data of **1** and **2** were collected using a Stoe IPDS II diffractometer with graphite-monochromated MoKα radiation. The data were corrected for Lorentz and polarization effects. The structures were solved by direct methods using SIR97 (ref. 21) and refined by full-matrix least-square techniques against F_0^2 (SHELXL-97 (ref. 22)). The hydrogen atoms were included at calculated positions with fixed displacement parameters, and allowed to ride their parent atoms. All non-hydrogen atoms were refined anisotropically. ORTEP-III[23] was used for the structure representation and SCHAKAL-99 (ref. 24) for the representation of the molecular packing. CCDC 1053320 (**1**) and 1053319 (**2**) contain the supplementary crystallographic data for this paper and can be obtained free of charge from the Cambridge Crystallographic Data Centre *via* http://www.ccdc.cam.ac.uk/data_request/cif.

Magnetic measurements

Magnetic measurements on the bulk materials were carried out using a SQUID MPMS-XL5 from Quantum Design with an applied field of 5000 G (**1**), 2000 G (**1**-TIESST and **2**), respectively, and in the temperature range from 400 to 10 K in the sweep (**1**) and settle (**2**) modes. The sample was prepared in a gelatine capsule held in a plastic straw. The raw data were corrected for the diamagnetic part of the sample holder and the diamagnetism of the organic ligand using tabulated Pascal's constants.

Conclusions

In this work we have presented two novel 1D iron(II) spin crossover coordination polymers with 3,3′-azopyridine as an axial ligand. The results from X-ray structure analysis revealed that the differences in the SCO behavior of the two complexes can be attributed to differences in the formation of hydrogen bonds in the molecular packing. The presence of free ligand molecules in the crystal packing of **1** supports the special perpendicular orientation of the polymer chains which again is associated with the unique magnetic properties. In contrast to the studies so far, where either the hysteresis width[5,6] or the completeness of the spin transition (quenching effects)[8,9] is influenced by the scan rate, we observe for complex **1** a combination of both effects.

Acknowledgements

Financial support from the German Science Foundation (SFB840; project A10) and the University of Bayreuth is acknowledged.

Notes and references

1 (*a*) *Spin-Crossover Materials*, ed. M. A. Halcrow, John Wiley & Sons Ltd, Chichester, 2013; (*b*) *Spin Crossover in Transition Metal Compounds I–III*, ed. P. Gütlich and H. Goodwin, Springer Berlin, Heidelberg, 2004, pp. 233–235.

2 (*a*) A. Tissot, *New J. Chem.*, 2014, **38**, 1840; (*b*) E. Coronado, J. R. Galán-Mascarós, M. Monrabal-Capilla, J. García-Martínez and P. Pardo-Ibáñez, *Adv. Mater.*, 2007, **19**, 1359–1361; (*c*) F. Volatron, L. Catala, E. Rivière, A. Gloter, O. Stéphan and T. Mallah, *Inorg. Chem.*, 2008, **47**, 6584–6586; (*d*) I. Boldog, A. B. Gaspar, V. Martínez, P. Pardo-Ibañez, V. Ksenofontov, A. Bhattacharjee, P. Gütlich and J. A. Real, *Angew. Chem.*, 2008, **120**, 6533–6537.

3 (*a*) M. Cavallini, I. Bergenti, S. Milita, G. Ruani, I. Salitros, Z.-R. Qu, R. Chandrasekar and M. Ruben, *Angew. Chem.*, 2008, **120**, 8724–8728; (*b*) C. Thibault, G. Molnár, L. Salmon, A. Bousseksou and C. Vieu, *Langmuir*, 2010, **26**, 1557–1560; (*c*) A. D. Naik, L. Stappers, J. Snauwaert, J. Fransaer and Y. Garcia, *Small*, 2010, **6**, 2842–2846; (*d*) Y. Raza, F. Volatron, S. Moldovan, O. Ersen, V. Huc, C. Martini, F. Brisset, A. Gloter, O. Stephan, A. Bousseksou, L. Catala and T. Mallah, *Chem. Commun.*, 2011, **47**, 11501–11503; (*e*) C. Göbel, T. Palamarciuc, C. Lochenieand and B. Weber, *Chem. – Asian J.*, 2014, **9**, 2232–2238.

4 (*a*) S. Titos-Padilla, J. M. Herrera, X.-W. Chen, J. J. Delgado and E. Colacio, *Angew. Chem., Int. Ed.*, 2011, **50**, 3290–3293; (*b*) L. Salmon, G. Molnár, D. Zitouni, C. Quintero, C. Bergaud, J.-C. Micheau and A. Bousseksou, *J. Mater. Chem.*, 2010, **20**, 5499; (*c*) A. B. Gaspar and M. Seredyuk, *Coord. Chem. Rev.*, 2014, **268**, 41–58.

5 R. Kulmaczewski, J. Olguín, J. A. Kitchen, H. L. C. Feltham, G. N. L. Jameson, J. L. Tallon and S. Brooker, *J. Am. Chem. Soc.*, 2014, **136**, 878–881.

6 R. G. Miller, S. Narayanaswamy, J. L. Tallon and S. Brooker, *New J. Chem.*, 2014, **38**, 1932.

7 M. Seredyuk, M. C. Muñoz, M. Castro, T. Romero-Morcillo, A. B. Gaspar and J. A. Real, *Chem. – Eur. J.*, 2013, **19**, 6591–6596.

8 V. A. Money, C. Carbonera, J. Elhaïk, M. A. Halcrow, J. A. K. Howard and J.-F. Létard, *Chem. – Eur. J.*, 2007, **13**, 5503–5514.

 This journal is © The Royal Society of Chemistry 2015

Open Access Article. Published on 22 May 2015. Downloaded on 8/18/2024 12:57:07 AM.
This article is licensed under a Creative Commons Attribution 3.0 Unported Licence.

9 N. F. Sciortino, S. M. Neville, C. Desplanches, J.-F. Létard, V. Martinez, J. A. Real, B. Moubaraki, K. S. Murray and C. J. Kepert, *Chem. – Eur. J.*, 2014, **20**, 7448–7457.

10 (*a*) W. Bauer, C. Lochenieand and B. Weber, *Dalton Trans.*, 2014, **43**, 1990–1999; (*b*) C. Lochenie, W. Bauer, A. P. Railliet, S. Schlamp, Y. Garcia and B. Weber, *Inorg. Chem.*, 2014, **53**, 11563–11572; (*c*) R. Nowak, W. Bauer, T. Ossianderand and B. Weber, *Eur. J. Inorg. Chem.*, 2013, 975–983.

11 (*a*) W. Bauer, W. Scherer, S. Altmannshoferand and B. Weber, *Eur. J. Inorg. Chem.*, 2011, 2803–2818; (*b*) C. Baldé, W. Bauer, E. Kaps, C. Desplanches, G. Chastanet, B. Weber and J.-F. Létard, *Eur. J. Inorg. Chem.*, 2013, 2744–2750.

12 W. Bauer, T. Ossiander and B. Weber, *Z. Naturforsch., B: J. Chem. Sci.*, 2010, 323–328.

13 E.-G. Jäger, E. Häussler, M. Rudolph and A. Schneider, *Z. Anorg. Allg. Chem.*, 1985, **525**, 67–85.

14 S. Thies, H. Sell, C. Schütt, C. Bornholdt, C. Näther, F. Tuczekand and R. Herges, *J. Am. Chem. Soc.*, 2011, **133**, 16243–16250.

15 G. Spaleniak, Z. Daszkiewicz and J. Kyzioł, *Chem. Pap.*, 2009, **63**, 313–322.

16 (*a*) B. Weber, *Coord. Chem. Rev.*, 2009, **253**, 2432–2449; (*b*) B. Weber and F.-A. Walker, *Inorg. Chem.*, 2007, **46**, 6794–6803.

17 S. Schlamp, P. Thoma and B. Weber, *Chem. – Eur. J.*, 2014, **20**, 6462–6473.

18 W. Bauer, T. Pfaffeneder, K. Achterhold and B. Weber, *Eur. J. Inorg. Chem.*, 2011, 3183–3192.

19 B. Weber, W. Bauer, T. Pfaffeneder, M. M. Dîrtu, A. D. Naik, A. Rotaruand and Y. Garcia, *Eur. J. Inorg. Chem.*, 2011, 3193–3206.

20 T. M. Pfaffeneder, S. Thallmair, W. Bauer and B. Weber, *New J. Chem.*, 2011, **35**, 691–700.

21 A. Altomare, M. C. Burla, M. Camalli, G. L. Cascarano, C. Giacovazzo, A. Guagliardi, A. G. G. Moliterni, G. Polidoriand and R. Spagna, *J. Appl. Crystallogr.*, 1999, **32**, 115–119.

22 G. Sheldrick, *Acta Crystallogr., Sect. A: Found. Crystallogr.*, 2008, **64**, 112–122.

23 (*a*) C. K. Johnson and M. N. Burnett, *ORTEP-III*, Oak-Ridge National Laboratory, Oak-Ridge, TN, 1996; (*b*) L. Farrugia, *J. Appl. Crystallogr.*, 1997, **30**, 565.

24 E. Keller, *Schakal-99*, University of Freiburg, Freiburg, Germany, 1999.